DALTON

Synthesis and properties of ligand-bridged dinuclear complexes containing *trans*-bis[*o*-phenylenebis(dimethylarsine)]-chlororuthenium(II) centres

Benjamin J. Coe,*,†,[a] Samar Hayat,[a] Roy L. Beddoes,[a] Madeleine Helliwell,[a] John C. Jeffery,[b] Stuart R. Batten[b] and Peter S. White[c]

[a] *Department of Chemistry, University of Manchester, Oxford Road, Manchester M13 9PL, UK*
[b] *Department of Chemistry, University of Bristol, Cantock's Close, Bristol BS8 1TS, UK*
[c] *Department of Chemistry, University of North Carolina, Chapel Hill, North Carolina 27599-3290, USA*

The series of mononuclear salts *trans*-[RuCl(pdma)$_2$(L–L)]PF_6 [pdma = *o*-phenylenebis(dimethylarsine); L–L = 4,4′-bipyridine (4,4′-bipy) **2**, fumaronitrile (fmn) **4**, di-4-pyridyl disulfide (dpds) **9** or *trans*-1,2-bis(4-pyridyl)ethylene (bpe) **11**] have been synthesized by reaction of *trans*-[RuCl(pdma)$_2$(NO)][PF_6]$_2$ with 1 equivalent of NaN_3 in acetone at room temperature followed by reflux with an excess of L–L in butan-2-one. The salt *trans*-[RuCl(pdma)$_2$(C_5H_5NS)]PF_6 **6** (C_5H_5NS = pyridine-4-thione) was prepared similarly by using pyridine-4-thiol, and *trans*-[RuCl(pdma)$_2$(C_5H_4NSH)]PF_6 **8** (C_5H_4NSH = pyridine-4-thiol) was produced upon prolonged reflux of **9** in butan-2-one. Salts **6** and **8** are readily deprotonated by aqueous NaOH to give *trans*-[RuCl(pdma)$_2$(C_5H_4NS)] **7** and **10**. The dinuclear salts *trans*-[{RuCl(pdma)$_2$}$_2$(μ-L–L)][PF_6]$_2$ [L–L = pyrazine (pyz) **1**, 4,4′-bipy **3**, fmn **5** or bpe **12**] have been synthesized by reaction of *trans*-[RuCl(pdma)$_2$(NO)][PF_6]$_2$ with 1 equivalent of NaN_3 followed by reflux with 1 equivalent of the monometallic salts *trans*-[RuCl(pdma)$_2$(pyz)]PF_6, **2**, **4** or **11**, respectively, in butan-2-one. The dimer *trans*-[{RuCl(pdma)$_2$}$_2$(μ-dpds)][I_3]$_2$ **13** was prepared by oxidation of **8** with iodine in Me_2SO at room temperature. Single-crystal structures of **1**, **3**, **6** and **13** have been determined, and the extent of intermetallic electronic coupling in the dimers **1**, **3**, **5**, **12** and **13** is assessed using cyclic voltammetry.

The study of intermetallic electronic interactions in ligand-bridged, di- and poly-nuclear transition-metal complexes has long attracted great academic interest. In particular, the celebrated Creutz–Taube ion, [$(NH_3)_5$Ru(pyz)Ru$(NH_3)_5$]$^{5+}$ (pyz = pyrazine),[1] and other mixed-valence complexes[2] have been extensively investigated using various physicochemical techniques. This has led to a well developed understanding of the factors which influence the electronic properties of ligand-bridged complexes, particularly those of ruthenium.[3]

It has recently become apparent that mixed-valence complexes have potential for practical applications in the emerging field of 'molecular electronics', as components of molecular-scale wires or switches.[3,4] In order for this promise to be realized there is a pressing need for synthetic work to create new, potentially exploitable complexes.

Almost without exception, existing ligand-bridged complexes are ill suited towards structural extension because they possess a *cis* geometry, *e.g. cis*-[{RuCl(bipy)$_2$}$_2$(μ-pyz)]$^{2+}$ (bipy = 2,2′-bipyridine).[5] The incorporation of functional, polynuclear metal complex units into active assemblies ideally requires derivatization of complexes having a *trans* geometry, allowing precisely defined 'connections' to be made at the molecular level. Few ligand-bridged complexes having a *trans* structure are known, particularly featuring substitution-labile terminal ligands such as chloride.

Di- and tri-nuclear ligand-bridged complexes based on *trans*-{Ru(py)$_4$}$^{2+}$ (py = pyridine) centres, exhibiting marked intermetallic interactions, have recently been prepared using *trans*-[RuCl(py)$_4$(NO)][PF_6]$_2$ as a precursor.[6,7] Related complexes containing the *trans*-{RuCl(pdma)$_2$}$^+$ centre [pdma = *o*-phenylenebis(dimethylarsine)] are attractive for synthetic investigations because (*i*) this represents a highly stable, bis-chelate unit bearing potentially labile chloride ligands, and (*ii*) the precursor *trans*-[RuCl(pdma)$_2$(NO)][PF_6]$_2$ has already been used to prepare mononuclear complexes *trans*-[RuCl(pdma)$_2$(L)]$^+$ (L = py, *etc*.).[8] The objectives of this study are the synthesis and characterization of a series of dinuclear ruthenium(II) complexes, *trans*-[{RuCl(pdma)$_2$}$_2$(μ-L–L)]$^{2+}$, which have potential both for generation of mixed-valence forms and for extension in one dimension *via* chloride substitution.

Experimental

Materials and procedures

The compound $RuCl_3$·$2H_2O$ was supplied by Johnson Matthey plc and pdma was obtained from Dr P. G. Edwards, University of Wales College of Cardiff. The salts *trans*-[RuCl(pdma)$_2$(NO)][PF_6]$_2$[9] and *trans*-[RuCl(pdma)$_2$(pyz)]PF_6[8] were prepared according to published procedures. All other reagents were obtained commercially and used as supplied. All reactions were conducted under an argon atmosphere. Products were dried at room temperature in a vacuum desiccator ($CaSO_4$) for *ca*. 24 h prior to characterization.

Physical measurements

Proton NMR spectra were recorded on a Varian Gemini 200 spectrometer and all shifts are referenced to $SiMe_4$. The fine splitting of pyridyl AA′BB′ patterns is ignored and the signals are reported as simple doublets, with *J* values referring to the two most intense peaks. Elemental analyses were performed by the Microanalytical Laboratory, University of Manchester. Infrared spectra were obtained as KBr discs with an ATI Mattson Genesis Series FTIR instrument, UV/VIS spectra using a Hewlett-Packard 8452A diode-array spectrophotometer and FAB mass spectra using a Kratos Concept spectrometer with a

† E-Mail: b.coe@man.ac.uk

6–8 keV (1 eV ≈ 1.60×10^{-19} J) Xe atom beam and 3-nitrobenzyl alcohol as matrix.

Cyclic voltammetric measurements were carried out using an EG&G PAR model 173 potentiostat/galvanostat with a model 175 universal programmer. A single-compartment cell was used with the saturated calomel reference electrode (SCE) separated by a salt bridge from the platinum-bead working electrode and platinum-wire auxiliary electrode. Acetonitrile (HPLC grade) was used as received and tetra-*n*-butylammonium hexafluorophosphate, twice recrystallized from ethanol and dried *in vacuo*, as supporting electrolyte. Solutions containing *ca.* 10^{-3} mol dm^{-3} analyte (0.1 mol dm^{-3} electrolyte) were deaerated by purging with N_2. All $E_{\frac{1}{2}}$ values were calculated from $(E_{pa} + E_{pc})/2$ at a scan rate of 200 mV s^{-1}.

Syntheses

***trans*-[{RuCl(pdma)$_2$}$_2$(μ-pyz)][PF$_6$]$_2$ 1.** A solution of *trans*-[RuCl(pdma)$_2$(NO)][PF$_6$]$_2$ (100 mg, 0.097 mmol) and NaN_3 (6.5 mg, 0.100 mmol) in acetone (5 cm^3) was stirred at room temperature for 2 h. Butan-2-one (10 cm^3) and *trans*-[RuCl(pdma)$_2$(pyz)]PF$_6$ (91 mg, 0.097 mmol) were added and the acetone removed *in vacuo*. The solution was heated at reflux in the dark for 2 h. After cooling in a refrigerator, the purple precipitate was filtered off and washed with butan-2-one. The product was dissolved in acetonitrile (5 cm^3) and precipitated by addition of aqueous NH_4PF_6. The purple precipitate was filtered off, washed with water and dried. It was recrystallized by precipitation from acetonitrile–diethyl ether to afford a deep purple solid: yield 91 mg, 53%. $\delta_H(CD_3CN)$ 8.03 (8 H, m, 4 × C_6H_2), 7.71 (8 H, m, 4 × C_6H_2), 6.68 (4 H, s, $C_4H_4N_2$), 1.73 (24 H, s, 8 × AsMe) and 1.43 (24 H, s, 8 × AsMe) (Found: C, 29.55; H, 3.65; N, 1.65. Calc. for $C_{44}H_{68}As_8Cl_2F_{12}N_2P_2Ru_2$: C, 29.55; H, 3.85; N, 1.55%).

***trans*-[RuCl(pdma)$_2$(4,4′-bipy)]PF$_6$ 2.** This salt was prepared in similar fashion to that for **1** by using 4,4′-bipyridine (610 mg, 3.91 mmol) in place of *trans*-[RuCl(pdma)$_2$(pyz)]PF$_6$. After heating at reflux for 2 h without protection from light the bright golden solution was cooled to room temperature and diethyl ether was added. The golden precipitate was filtered off, washed with diethyl ether and dried. It was purified by precipitation from acetone–aqueous NH_4PF_6 then from acetone–diethyl ether to afford a golden solid: yield 90 mg, 92%. $\delta_H(CD_3COCD_3)$ 8.63 (2 H, d, J = 6.2, C_5H_4N), 8.33 (4 H, m, 2 × C_6H_2), 7.85 (4 H, m, 2 × C_6H_2), 7.76 (2 H, d, J = 7.0, C_5H_4N), 7.58 (2 H, d, J = 6.2, C_5H_4N), 7.50 (2 H, d, J = 6.9 Hz, C_5H_4N), 1.92 (12 H, s, 4 × AsMe) and 1.81 (12 H, s, 4 × AsMe) (Found: C, 35.35; H, 3.6; N, 2.35. Calc. for $C_{30}H_{40}As_4ClF_6N_2PRu$: C, 35.7; H, 4.0; N, 2.75%).

***trans*-[{RuCl(pdma)$_2$}$_2$(μ-4,4′-bipy)][PF$_6$]$_2$ 3.** This salt was prepared and purified in similar fashion to that for **1** by using *trans*-[RuCl(pdma)$_2$(NO)][PF$_6$]$_2$ (75 mg, 0.073 mmol), NaN_3 (4.9 mg, 0.075 mmol) and **2** (74 mg, 0.073 mmol) in place of *trans*-[RuCl(pdma)$_2$(pyz)]PF$_6$. The product was obtained as a red-orange solid: yield 83 mg, 61%. $\delta_H(CD_3CN)$ 8.14 (8 H, m, 4 × C_6H_2), 7.78 (8 H, m, 4 × C_6H_2), 7.37 (4 H, d, J = 6.9, C_5H_4N), 6.87 (4 H, d, J = 6.9 Hz, C_5H_4N), 1.77 (24 H, s, 8 × AsMe) and 1.54 (24 H, s, 8 × AsMe) (Found: C, 32.5; H, 4.0; N, 1.5. Calc. for $C_{50}H_{72}As_8Cl_2F_{12}N_2P_2Ru_2$: C, 32.25; H, 3.9; N, 1.5%).

***trans*-[RuCl(pdma)$_2$(fmn)]PF$_6$ 4.** This salt was prepared and purified in similar fashion to that for **2** by using fumaronitrile (313 mg, 4.01 mmol) in place of 4,4′-bipyridine. The product was obtained as a golden solid: yield 85 mg, 94%. $\delta_H(CD_3COCD_3)$ 8.23 (4 H, m, 2 × C_6H_2), 7.78 (4 H, m, 2 × C_6H_2), 6.76 (1 H, d, J = 16.6, CH), 6.48 (1 H, d, J = 16.5 Hz, CH) and 1.93 (24 H, s, 8 × AsMe). ν(C≡N) 2193vs cm^{-1} (Found: C, 31.1; H, 3.8; N, 3.1. Calc. for $C_{24}H_{34}As_4ClF_6N_2PRu$: C, 30.95; H, 3.7; N, 3.0%).

***trans*-[{RuCl(pdma)$_2$}$_2$(μ-fmn)][PF$_6$]$_2$ 5.** This salt was prepared and purified in a similar fashion to that for **3** by using **4** (68 mg, 0.073 mmol) in place of **2**. The product was obtained as an orange solid: yield 60 mg, 46%. $\delta_H(CD_3CN)$ 8.04 (8 H, m, 4 × C_6H_2), 7.70 (8 H, m, 4 × C_6H_2), 5.70 (2 H, s, CH=CH), 1.77 (24 H, s, 8 × AsMe) and 1.63 (24 H, s, 8 × AsMe). ν(C≡N) 2200s cm^{-1} (Found: C, 29.7; H, 3.75; N, 1.7. Calc. for $C_{44}H_{66}As_8Cl_2F_{12}N_2P_2Ru_2$: C, 29.6; H, 3.75; N, 1.55%). Owing to the partial solubility of the product in butan-2-one, 42 mg of pure **5** were obtained from the reaction filtrate solution after precipitation with diethyl ether and recyrstallization from acetonitrile–diethyl ether: total yield 102 mg, 78%.

***trans*-[RuCl(pdma)$_2$(C$_5$H$_5$NS)]PF$_6$ 6.** This salt was prepared in similar fashion to that for **2** by using *trans*-[RuCl(pdma)$_2$(NO)][PF$_6$]$_2$ (200 mg, 0.194 mmol), NaN_3 (13 mg, 0.200 mmol) and pyridine-4-thiol (550 mg, 4.95 mmol) in place of 4,4′-bipyridine. Addition of diethyl ether to the cooled orange solution caused rapid precipitation of excess of thiol which was filtered off. Addition of further diethyl ether to the filtrate solution afforded an orange precipitate which was filtered off, washed with diethyl ether and dried. The product was purified by reprecipitation as for **2** to afford an orange-brown solid: yield 168 mg, 90%. $\delta_H(CD_3COCD_3)$ 8.23 (4 H, m, 2 × C_6H_2), 7.78 (4 H, m, 2 × C_6H_2), 7.33 (2 H, d, J = 7.3, C_5H_4N), 6.57 (2 H, d, J = 7.3 Hz, C_5H_4N), 1.83 (12 H, s, 4 × AsMe) and 1.82 (12 H, s, 4 × AsMe). ν(N–H) 3353m, ν(C=C) 1625s and ν(C=S) 1116m cm^{-1} (Found: C, 31.4; H, 3.95; N, 1.45; S, 3.1. Calc. for $C_{25}H_{37}As_4ClF_6NPRuS$: C, 31.1; H, 3.85; N, 1.45; S, 3.3%).

***trans*-[RuCl(pdma)$_2$(C$_5$H$_4$NS)] 7.** Aqueous NaOH solution (0.2 mol dm^{-3}, 20 cm^3) was added dropwise to a solution of salt **6** (120 mg, 0.124 mmol) in acetone (5 cm^3). The golden-orange solution immediately faded and a pale precipitate formed. This was filtered off, washed with water and dried. Reprecipitation from dichloromethane–diethyl ether afforded a pale golden-orange solid: yield 88 mg, 86%. $\delta_H(CDCl_3)$ 7.92 (4 H, m, 2 × C_6H_2), 7.63 (4 H, m, 2 × C_6H_2), 7.39 (2 H, d, J = 6.2, C_5H_4N), 6.28 (2 H, d, J = 6.2 Hz, C_5H_4N), 1.72 (12 H, s, 4 × AsMe) and 1.70 (12 H, s, 4 × AsMe) (Found: C, 36.8; H, 4.55; N, 1.65; S, 3.85. Calc. for $C_{25}H_{36}As_4ClNRuS$: C, 36.65; H, 4.45; N, 1.7; S, 3.9%).

***trans*-[RuCl(pdma)$_2$(C$_5$H$_4$NSH)]PF$_6$ 8.** This salt was obtained in crude form in similar fashion to that for **2** by using *trans*-[RuCl(pdma)$_2$(NO)][PF$_6$]$_2$ (125 mg, 0.122 mmol), NaN_3 (8.1 mg, 0.125 mmol) and di-4-pyridyl disulfide (dpds) (274 mg, 1.24 mmol) in place of 4,4′-bipyridine. It was purified by precipitation from acetonitrile–diethyl ether and then from acetonitrile–aqueous NH_4PF_6, followed by recrystallization from acetonitrile–diethyl ether to afford a yellow microcrystalline solid: yield 88 mg, 75%. $\delta_H(CD_3CN)$ 8.16 (4 H, m, 2 × C_6H_2), 7.80 (4 H, m, 2 × C_6H_2), 7.10 (2 H, d, J = 7.0, C_5H_4N), 6.70 (2 H, d, J = 7.0 Hz, C_5H_4N), 1.80 (12 H, s, 4 × AsMe) and 1.50 (12 H, s, 4 × AsMe) (Found: C, 31.3; H, 3.85; N, 1.6; S, 3.55. Calc. for $C_{25}H_{37}As_4ClF_6NPRuS$: C, 31.1; H, 3.85; N, 1.45; S, 3.3%).

***trans*-[RuCl(pdma)$_2$(dpds)]PF$_6$ 9.** This salt was obtained in crude form in similar fashion to that for **8** but with a reflux time of 10 min. It was purified by reprecipitation from acetone–diethyl ether to afford a golden solid: yield 110 mg, 84%. $\delta_H(CD_3COCD_3)$ 8.41 (2 H, d, J = 6.2, C_5H_4N), 8.27 (4 H, m, 2 × C_6H_2), 7.80 (4 H, m, 2 × C_6H_2), 7.55 (2 H, d, J = 7.0, C_5H_4N), 7.33 (2 H, d, J = 6.2, C_5H_4N), 7.22 (2 H, d, J = 7.0 Hz, C_5H_4N), 1.88 (12 H, s, 4 × AsMe) and 1.74 (12 H, s, 4 × AsMe)

(Found: C, 33.15; H, 3.9; N, 3.05; S, 6.45. Calc. for $C_{30}H_{40}As_4ClF_6N_2PRuS_2$: C, 33.55; H, 3.75; N, 2.6; S, 5.95%).

***trans*-[RuCl(pdma)$_2$(C$_5$H$_4$NS)] 10.** Aqueous NaOH solution (0.2 mol dm^{-3}, 15 cm^3) was added dropwise to a solution of salt **8** (50 mg, 0.052 mmol) in acetonitrile (3 cm^3). The yellow precipitate was filtered off, washed with water and dried: yield 41.5 mg, 98%. ν(C=C) 1590s, ν(C=S) 1120s cm^{-1} (Found: C, 36.0; H, 4.25; N, 1.55; S, 3.6. Calc. for $C_{25}H_{36}As_4ClNRuS\cdot H_2O$: C, 35.9; H, 4.6; N, 1.65; S, 3.85%).

***trans*-[RuCl(pdma)$_2$(bpe)]PF$_6$ 11.** This salt was prepared in similar fashion to that for **2** by using *trans*-[RuCl(pdma)$_2$(NO)][PF$_6$]$_2$ (125 mg, 0.122 mmol), NaN_3 (8.1 mg, 0.125 mmol) and *trans*-1,2-bis(4-pyridyl)ethylene (bpe) (885 mg, 4.86 mmol) in place of 4,4′-bipyridine. Prior to precipitation from acetone–aqueous NH_4PF_6 the excess of bpe was removed by two reprecipitations from acetone–diethyl ether. The product was obtained as an orange microcrystalline solid: yield 112 mg, 87%. $\delta_H(CD_3COCD_3)$ 8.53 (2 H, d, J = 6.2, C_5H_4N), 8.32 (4 H, m, 2 × C_6H_2), 7.85 (4 H, m, 2 × C_6H_2), 7.61 (2 H, d, J = 6.9, C_5H_4N), 7.43 (2 H, d, J = 6.1, C_5H_4N), 7.34 (2 H, m, CH=CH), 7.25 (2 H, d, J = 6.8 Hz, C_5H_4N), 1.90 (12 H, s, 4 × AsMe) and 1.80 (12 H, s, 4 × AsMe) (Found: C, 37.7; H, 4.15; N, 2.8. Calc. for $C_{32}H_{42}As_4ClF_6N_2PRu\cdot0.5C_3H_6O$: C, 37.8; H, 4.25; N, 2.65%).

***trans*-[{RuCl(pdma)$_2$}$_2$(μ-bpe)][PF$_6$]$_2$ 12.** This salt was prepared and purified in similar fashion to that for **3** by using **11** (75.5 mg, 0.073 mmol) in place of **2**. The product was obtained as a burgundy solid: yield 91 mg, 66%. $\delta_H(CD_3CN)$ 8.15 (8 H, m, 4 × C_6H_2), 7.78 (8 H, m, 4 × C_6H_2), 7.27 (4 H, d, J = 6.7, C_5H_4N), 6.89 (2 H, s, CH=CH), 6.79 (4 H, d, J = 6.8 Hz, C_5H_4N), 1.78 (24 H, s, 8 × AsMe) and 1.56 (24 H, s, 8 × AsMe) (Found: C, 33.25; H, 3.8; N, 1.35. Calc. for $C_{52}H_{74}As_8Cl_2F_{12}N_2P_2Ru_2$: C, 33.05; H, 3.95; N, 1.5%).

***trans*-[{RuCl(pdma)$_2$}$_2$(μ-dpds)][I$_3$]$_2$ 13.** A solution of salt **8** (112 mg, 0.116 mmol) and iodine (37 mg, 0.146 mmol) in Me_2SO (2 cm^3) was left to stand at room temperature in the dark for 63 h. Acetone and diethyl ether were added, and the golden precipitate was filtered off and washed with diethyl ether. The solid was washed with acetonitrile to remove unchanged **8** and then dried. It was purified by reprecipitation from Me_2SO–acetone–diethyl ether. The golden brown precipitate was filtered off, washed with acetonitrile then diethyl ether and dried: yield 52 mg, 37%. $\delta_H(CD_3SOCD_3)$ 8.29 (8 H, m, 4 × C_6H_2), 7.81 (8 H, m, 4 × C_6H_2), 7.18 (4 H, d, J = 6.8, C_5H_4N), 7.01 (4 H, d, J = 6.5 Hz, C_5H_4N), 1.79 (24 H, s, 8 × AsMe) and 1.54 (24 H, s, 8 × AsMe) (Found: C, 25.7; H, 3.1; N, 1.75; S, 3.4. Calc. for $C_{50}H_{72}As_8Cl_2I_6N_2Ru_2S_2\cdot C_2H_3N$: C, 25.6; H, 3.1; N, 1.7; S, 2.65%).

Crystallography

Crystals of *trans*-[{RuCl(pdma)$_2$}$_2$(μ-pyz)][PF$_6$]$_2$·2MeCN·Et$_2$O (**1**·2MeCN·Et$_2$O), *trans*-[{RuCl(pdma)$_2$}$_2$(μ-4,4′-bipy)][PF$_6$]$_2$·2MeCN·Et$_2$O (**3**·2MeCN·Et$_2$O) and **6** were grown by diffusion of diethyl ether vapour into acetonitrile solutions at room temperature. Crystals of *trans*-[{RuCl(pdma)$_2$}$_2$(μ-dpds)][I$_3$]$_2$·2MeCN (**13**·2MeCN) were grown by iodine oxidation of **8** in 1% Me_2SO–acetonitrile solution, the poor solubility of **13** in acetonitrile causing crystallization.

A dark red crystal of salt **1**·2MeCN·Et$_2$O of dimensions 0.30 × 0.30 × 0.35 mm was selected for diffraction study and data were collected on a Rigaku AFC6S diffractometer at low temperature. The structure was solved using the NRCVAX suite of programs,[10] and refined using full-matrix least squares on F_o for all unique reflections. Data were corrected for absorption with maximum and minimum transmission factors of 0.43 and 0.27. The non-hydrogen atoms were refined anisotropically and hydrogen atoms were included in idealized positions. Two molecules of acetonitrile and one of diethyl ether are present for every complex cation.

A red prismatic crystal of salt **3**·2MeCN·Et$_2$O of dimensions 0.40 × 0.20 × 0.15 mm was selected for diffraction study and data were collected using a Rigaku RAXIS II imaging-plate area detector at low temperature. The structure was solved by direct methods with DIRDIF 94,[11] and refined using full-matrix least squares on F_o for all unique reflections (TEXSAN)[12] with correction for Lorentz-polarization effects. No correction was made for absorption. The non-hydrogen atoms were refined anisotropically and hydrogen atoms were included in idealized positions. The asymmetric unit contains half of the complex cation, *trans*-[RuCl(pdma)$_2$(NC$_5$H$_4$)]$^+$, one PF_6^- anion and two volumes of solvent which appear to be one molecule of acetonitrile and half a molecule of diethyl ether, each disordered over two sites. The atoms of these solvent molecules were refined isotropically and their hydrogens were not included.

An orange tabular crystal of salt **6** of dimensions 0.05 × 0.17 × 0.35 mm was mounted on a glass fibre and data were collected on a Rigaku AFC5R diffractometer at ambient temperature. The structure was solved by direct methods with SHELXS 86,[13] and refined using full-matrix least squares on F_o for all unique reflections (TEXSAN)[12] with correction for Lorentz-polarization factors. Data were corrected for absorption using the program DIFABS,[14] with maximum and minimum transmission factors of 1.00 and 0.61. The non-hydrogen atoms were refined anisotropically and hydrogen atoms were included in idealized positions.

A brown prismatic crystal of salt **13**·2MeCN of dimensions 0.60 × 0.45 × 0.40 mm was mounted on a glass fibre and data were collected on a Siemens SMART CCD area-detector three-circle diffractometer at low temperature. For three settings of φ, narrow data 'frames' were collected for 0.3° increments in ω. A total of 1271 frames were collected, affording rather more than a hemisphere of data. At the end of data collection the first 50 frames were recollected to establish that crystal decay had not taken place. The substantial redundancy in data allows empirical absorption corrections to be applied using multiple measurements of equivalent reflections. Data frames were collected for 10 s per frame giving an overall data-collection time of *ca.* 7 h. The data frames were integrated using SAINT.[15] The structure was solved by direct methods and refined by full-matrix least squares on all F_o^2 data using Siemens SHELXTL 5.03.[15] All non-hydrogen atoms were refined anisotropically. All hydrogen atoms were included in calculated positions with isotropic thermal parameters *ca.* 1.2 × (aromatic CH) or 1.5 × (Me) the equivalent isotropic thermal parameters of their parent carbon atoms. All calculations were carried out on Silicon Graphics Indy or Indigo computers. The complex cation has crystallographically imposed two-fold symmetry. The asymmetric unit contains half of the complex cation, *trans*-[RuCl(pdma)$_2$(NC$_5$H$_4$S)]$^+$, and one I_3^- anion and one molecule of acetonitrile in general positions.

The ORTEP[16] diagrams showing views of the complexes are given in Figs. 1–4. Crystallographic data and refinement details are presented in Table 3, selected bond distances and angles in Tables 4–7. Atomic coordinates, thermal parameters, and bond lengths and angles have been deposited at the Cambridge Crystallographic Data Centre (CCDC). See Instructions for Authors, *J. Chem. Soc., Dalton Trans.*, 1997, Issue 1. Any request to the CCDC for this material should quote the full literature citation and the reference number 186/342.

Results and Discussion

Synthetic studies

The mononuclear salts **2**, **4** and **11** were synthesized using a previously developed procedure involving reaction of *trans*-

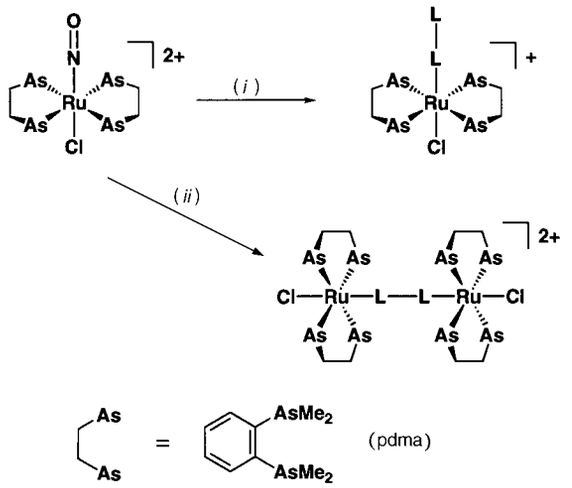

Scheme 1 Synthesis of the symmetric *trans*-{Ru(pdma)$_2$}$^{2+}$ complexes in **1**, **3**, **5** and **12** (*i*) (*a*) 1 equivalent NaN_3, (*b*) excess of L–L; (*ii*) as (*i*) (*a*) then 1 equivalent *trans*-[RuCl(pdma)$_2$(L–L)]$^+$

[RuCl(pdma)$_2$(NO)][PF$_6$]$_2$ with stoichiometric NaN_3 to generate *trans*-[RuCl(pdma)$_2$(N$_2$)]$^+$.[8] Treatment of the latter with an excess of the appropriate pro-ligand in refluxing butan-2-one gives *trans*-[RuCl(pdma)$_2$(L–L)]$^+$ [L–L = 4,4′-bipyridine **2**, fumaronitrile **4** or *trans*-1,2-bis(4-pyridyl)ethylene **11**] in almost quantitative yields. Reaction of **2**, **4** or **11** with stoichiometric *trans*-[RuCl(pdma)$_2$(N$_2$)]$^+$ affords the symmetrical dinuclear salts **3**, **5** and **12** in good yields. The dimer **1** was prepared similarly using the previously reported *trans*-[RuCl(pdma)$_2$-(pyz)]$^+$.[8] The synthetic strategy is summarized in Scheme 1.

Reaction of *trans*-[RuCl(pdma)$_2$(N$_2$)]$^+$ with di-4-pyridyl disulfide for a short period at reflux yields *trans*-[RuCl(pdma)$_2$-(dpds)]PF$_6$ **9** in high yield. Salt **9** has limited stability and upon prolonged reflux in butan-2-one is converted almost quantitatively into the nitrogen-bound pyridine-4-thiol salt, *trans*-[RuCl(pdma)$_2$(C$_5$H$_4$NSH)]PF$_6$ **8**, *via* disulfide cleavage. The reaction of **9** with stoichiometric *trans*-[RuCl(pdma)$_2$(N$_2$)]$^+$ is hence not a viable route to the dpds-bridged dimer complex, *trans*-[{RuCl(pdma)$_2$}$_2$(μ-dpds)]$^{2+}$. The latter was prepared in reasonable yield as the triiodide salt **13** by room-temperature oxidation of **8** with iodine in Me_2SO.

Treatment of *trans*-[RuCl(pdma)$_2$(N$_2$)]$^+$ with pyridine-4-thiol affords the sulfur-bound pyridine-4-thione salt *trans*-[RuCl-(pdma)$_2$(C$_5$H$_5$NS)]PF$_6$ **6**. This occurs because pyridine-4-thiol exists primarily as the pyridine-4-thione tautomer in solution,[17] rendering the thione sulfur a better donor site than the secondary amine nitrogen. Both **6** and **8** are quantitatively deprotonated by aqueous NaOH to afford the neutral complexes **7** and **10**, respectively. In both cases this induces tautomerization of the ligand (see below), as charge migrates to the site of coordination. Treatment of **7** with acetone–HCl gives quantitative recovery of **6**.* Complex **10** reverts to **8** on reaction with acetonitrile–HCl, but with significant decomposition.†

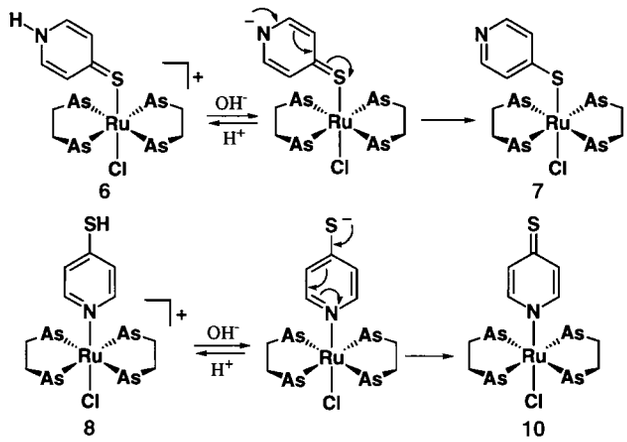

Scheme 2 pH-Controlled interconversion of complexes **6** and **7** and **8** and **10**

Infrared studies

The fumaronitrile salts **4** and **5** show strong ν(C≡N) bands, with a small high-energy shift of 10 cm^{-1} on bridging. The pyridine-4-thione salt **6** exhibits bands assigned to ν(N–H), ν(C=C) and ν(C=S) (at 1116 cm^{-1}), all of which are lost upon deprotonation to give **7**, as the ligand is converted into the thiolate form. The pyridine-4-thiol salt **8** does not show a ν(S–H) band. Upon deprotonation to give **10** a new, strong band assigned to ν(C=S) appears at 1120 cm^{-1}, showing that the ligand is converted into the thionate form. These structural changes are illustrated in Scheme 2.

Proton NMR studies

The benzene ring protons of the pdma ligands show AA′BB′ multiplets, characteristic of *ortho*-substituted rings, approximating to two sets of four signals. The presence of a single AA′BB′ pattern for each complex confirms the *trans* geometry. Singlets due to the $AsMe_2$ groups are also observed. All other ligands give the expected signals, particularly AA′BB′ patterns, approximating to two doublets, for 4-substituted pyridyl rings. The dimers show simplified spectra when compared to those of the monomers due to increased symmetry. No signals are observed for the amino or thiol protons in **6** or **8**, respectively.

FAB Mass spectrometric studies

All Ru-containing fragments are detected as broad isotope envelopes (Table 1). The most intense peaks within envelopes are reported, which may not correspond exactly with values calculated from relative atomic masses. Of the PF_6^- salts, most show the unfragmented $[M]^+$ parent ion including the anion(s), and all show the complex cation having lost one or two PF_6^- anions. The pyridine-4-thiol complex **8** dimerizes under the oxidizing conditions of FAB analysis, forming *trans*-[{RuCl-(pdma)$_2$}$_2$(μ-dpds)]$^{2+}$. All of the dimers *trans*-[{RuCl(pdma)$_2$}$_2$-(μ-L–L)]$^{2+}$ show fragments due to loss of the RuCl(pdma)$_2$L and RuCl(pdma)$_2$ units.

UV/VIS Studies

Spectra for all of the complexes were recorded in acetonitrile or Me_2SO and results are presented in Table 2, along with data for *trans*-[RuCl(pdma)$_2$(pyz)]PF$_6$.[8] for comparison purposes.

Intense, broad $d_\pi(Ru^{II}) \longrightarrow \pi^*(L)$ metal-to-ligand charge-transfer (m.l.c.t.) bands are observed in the region 370–570 nm for salts **1**–**5**, **8**, **9** and **11**–**13**. For the mononuclear complexes *trans*-[RuCl(pdma)$_2$(L–L)]$^+$ the m.l.c.t. energy increases in the order L–L = bpe < pyz < 4,4′-bipy < fmn < dpds, indicating a destabilization of the π* ligand acceptor LUMO (lowest unoccupied molecular orbital). In all cases except for L–L =

* Aqueous NaOH solution (0.2 mol dm^{-3}, 10 cm^3) was added dropwise to a solution of salt **6** (30 mg, 0.031 mmol) in acetone (2 cm^3). The pale precipitate was filtered off, washed with water and dried (25 mg). The solid was dissolved in HCl–acetone (1:1), and aqueous NH_4PF_6 was added. The orange precipitate was filtered off, washed with water and dried (29 mg, 97% recovery). The identity of the product as pure **6** was established by ^{1}H NMR spectroscopy.

† Aqueous NaOH solution (0.2 mol dm^{-3}, 10 cm^3) was added dropwise to a solution of salt **8** (30 mg, 0.031 mmol) in acetonitrile (2 cm^3). The yellow precipitate was filtered off, washed with water and dried (25 mg). The solid was dissolved in HCl–acetonitrile (1:1), and aqueous NH_4PF_6 was added. The yellow precipitate was filtered off, washed with water and dried (28 mg). This material was found to contain *ca.* 90% **8** by ^{1}H NMR spectroscopy. Recrystallization from acetonitrile–diethyl ether afforded pure **8** (22.5 mg, 75% recovery).

Table 1 Fast atom bombardment mass spectral data

	Fragment, m/z [a]				
Complex	$[M]^+$	$[M - PF_6^-]^+$	$[M - 2PF_6^-]^+$	$[M - 2PF_6^- - \{RuCl(pdma)_2\}^+]^+$	Others [b]
1	1786	1643	1498	789	750, $[RuCl(pdma)_2(NC_2H_2)]^+$
2	1010	865			
3	1864	1717	1573	865	787, $[RuCl(pdma)_2(NC_5H_4)]^+$
4		787			
5	1786	1641	1496	787	748, $[RuCl(pdma)_2(NC_2H)]^+$
6		820			
7	819				
8	1928	1784	1639	929	819, $[RuCl(pdma)_2(NC_5H_4S)]^+$
9		929			819, $[RuCl(pdma)_2(NC_5H_4S)]^+$
10	818				
11	1036	891			
12 [c]		1744	1601	890	799, $[RuCl(pdma)_2(NC_5H_4CH)]^+$
13					1763, $[M - I_5^-]^+$; 1636, $[M - 2I_3^-]^+$
					928, $[RuCl(pdma)_2(dpds)]^+$
					818, $[RuCl(pdma)_2(NC_5H_4S)]^+$

[a] Positive-ion mass spectra recorded using a 6–8 keV xenon-atom beam and 3-nitrobenzyl alcohol as matrix. [b] All complexes show an intense ion envelope at m/z 709 for $[RuCl(pdma)_2]^+$ and less intense envelopes at m/z 694, $[RuCl(pdma)_2 - Me]^+$ and 679, $[RuCl(pdma)_2 - 2Me]^+$. [c] $[M]^+$ not observed due to poor solubility.

Table 2 The UV/VIS and electrochemical data

	$E_{\frac{1}{2}}$/V *vs.* SCE (ΔE_p/mV) [a]			
Complex	$Ru^{III/II}$	Other waves	λ/nm (ε/dm^3 mol^{-1} cm^{-1}) [b]	Assignment
trans-$[RuCl(pdma)_2(pyz)]PF_6$ [8]	1.20 (70)	−1.50 [c]	220 (28 700)	π ⟶ π*
			256 (7000)	π ⟶ π*
			280 (sh) (2500)	π ⟶ π*
			422 (6100)	d_π ⟶ π*(pyz)
1 *trans*-$[\{RuCl(pdma)_2\}_2(\mu\text{-pyz})][PF_6]_2$	1.22 (65)	−1.01 (65)	220 (38 300)	π ⟶ π*
	1.54 (80)		268 (7700)	π ⟶ π*
			564 (34 200)	d_π ⟶ π*(pyz)
2 *trans*-$[RuCl(pdma)_2(4,4'\text{-bipy})]PF_6$	1.08 (60)	−1.51 [c]	212 (31 000)	π ⟶ π*
			226 (32 800)	π ⟶ π*
			418 (8400)	d_π ⟶ π*(4,4′-bipy)
3 *trans*-$[\{RuCl(pdma)_2\}_2(\mu\text{-}4,4'\text{-bipy})][PF_6]_2$	1.11 (95)	−1.19 (60)	214 (29 200)	π ⟶ π*
		−1.75 [c]	234 (35 400)	π ⟶ π*
			471 (20 900)	d_π ⟶ π*(4,4′-bipy)
4 *trans*-$[RuCl(pdma)_2(fmn)]PF_6$	1.31 (70)	−1.07 [c]	212 (28 200)	π ⟶ π*
			232 (32 200)	π ⟶ π*
			406 (11 200)	d_π ⟶ π*(fmn)
5 *trans*-$[\{RuCl(pdma)_2\}_2(\mu\text{-fmn})][PF_6]_2$	1.28 (60)	−0.92 [c]	216 (32 800)	π ⟶ π*
	1.38 (60)		234 (38 800)	π ⟶ π*
			464 (33 400)	d_π ⟶ π*(fmn)
6 *trans*-$[RuCl(pdma)_2(C_5H_5NS)]PF_6$	0.57 (70)	−0.61 (250)	218 (19 000)	π ⟶ π*
			238 (18 300)	π ⟶ π*
			296 (10 100)	π ⟶ π* (CH=CH)
			348 (4000)	π ⟶ d_π
			430 (9300)	π ⟶ d_π
			458 (8900)	π ⟶ d_π
7 *trans*-$[RuCl(pdma)_2(C_5H_4NS)]$	0.19 (65)		218 (33 300)	π ⟶ π*
			252 (16 300)	π ⟶ π*
			350 (8500)	π ⟶ d_π
8 *trans*-$[RuCl(pdma)_2(C_5H_4NSH)]PF_6$	1.07 (65)	−0.83 [c]	208 (57 300)	π ⟶ π*
			268 (28 400)	π ⟶ π*
			392 (5600)	d_π ⟶ π*(C_5H_4NSH)
9 *trans*-$[RuCl(pdma)_2(dpds)]PF_6$	1.10 (80)		218 (38 500)	π ⟶ π*
			264 (13 400)	π ⟶ π*
			382 (7100)	d_π ⟶ π*(dpds)
10 *trans*-$[RuCl(pdma)_2(C_5H_4NS)]$	1.13 [d]	0.53 [d]	300 (5300)	π ⟶ π*(CH=CH)
		0.85 [d]	366 (16 700)	π ⟶ d_π
11 *trans*-$[RuCl(pdma)_2(bpe)]PF_6$	1.06 (60)	−1.35 (60)	228 (33 900)	π ⟶ π*
		−1.75 [c]	292 (44 300)	π ⟶ π*(CH=CH)
			434 (14 300)	d_π ⟶ π*(bpe)
12 *trans*-$[\{RuCl(pdma)_2\}_2(\mu\text{-bpe})][PF_6]$	1.07 (80)	−1.14 [c]	224 (34 000)	π ⟶ π*
		−1.44 [c]	298 (33 200)	π ⟶ π*(CH=CH)
		−1.55 [c]	480 (27 400)	d_π ⟶ π*(bpe)
13 *trans*-$[\{RuCl(pdma)_2\}_2(\mu\text{-dpds})][I_3]_2$	1.12 (100)	0.43 [d]	298 (72 700)	π ⟶ π*
		0.66 (130)	370 (53 400)	d_π ⟶ π*(dpds)
		1.52 [d]		

[a] Using solutions *ca.* 10^{-3} mol dm^{-3} in complex and 0.1 mol dm^{-3} in $NBu^n_4PF_6$ at a platinum-bead working electrode with a scan rate of 200 mV s^{-1}. Ferrocene internal reference $E_{\frac{1}{2}} = 0.41$ V, $\Delta E_p = 60$ mV. Measured in acetonitrile, except for **9** and **13** measured in dmf. [b] Measured in acetonitrile, except for **10** and **13** measured in Me_2SO. [c] E_{pc} for an irreversible reduction process. [d] E_{pa} for an irreversible oxidation process.

dpds the m.l.c.t. bands are red-shifted upon dimer formation, with a concomitant increase in extinction by a factor of 2–3. Such a lowering in m.l.c.t. energy is commonly observed in dinuclear ligand-bridged complexes, and is attributed to a stabilization of the π* acceptor orbitals of the bridging ligand upon attachment of a second metal centre.[18] The m.l.c.t. band at 564 nm (ε = 34 200 dm^3 mol^{-1} cm^{-1}) for **1** compares with values of 570 nm (ε = 23 700 dm^3 mol^{-1} cm^{-1})[6] for *trans*-$[\{RuCl(py)_4\}_2(\mu\text{-pyz})]^{2+}$ and 547 nm (ε = 30 000 dm^3 mol^{-1} cm^{-1})[1] for $[\{Ru(NH_3)_5\}_2(\mu\text{-pyz})]^{4+}$ (in aqueous solution). In the case of L–L = dpds the m.l.c.t. absorption is slightly blue-shifted upon dimer formation, accompanied by an eight-fold increase in extinction. For the related complex $[\{Ru(NH_3)_5\}_2(\mu\text{-dpds})]^{4+}$ the m.l.c.t. band is red-shifted by 8 nm with respect to that of $[Ru(NH_3)_5(dpds)]^{2+}$.[19] The stronger colour of **13** with respect to **9** is due to a more intense tailing into the visible region; at 450 nm, ε = 6600 dm^3 mol^{-1} cm^{-1} for **13** (in Me_2SO) and ε = 1000 dm^3 mol^{-1} cm^{-1} for **9** (in MeCN).

The pyridine-4-thione salt **6** exhibits intense bands at 348, 430 and 458 nm, assigned to $p_\pi(S) \longrightarrow d_\pi(Ru^{II})$ ligand-to-metal charge-transfer (l.m.c.t.) excitations by comparison with related complexes.[20] Deprotonation of **6** to give **7** results in loss of the two visible bands, with only one remaining l.m.c.t. absorption at 350 nm. The pyridine-4-thionate complex **10** exhibits a single l.m.c.t. band at 366 nm.

In addition to the c.t. bands, all of the complexes show very intense, high-energy bands below 300 nm due to intraligand $\pi \longrightarrow \pi^*$ excitations. Bands in the region 290–300 nm for the bpe complexes **11** and **12** are assigned to $\pi \longrightarrow \pi^*$ excitations of the ethylene group, shifted to low energy by conjugation. The pyridine-4-thione salt **6** and the pyridine-4-thionate complex **10** exhibit analogous absorptions at 296 and 300 nm, respectively.

The dimers **1**, **3** and **12** are photosensitive in acetonitrile solution; exposure to ambient light for several hours causes complete loss of visible absorption, accompanied by the appearance of a new band at *ca*. 354 nm due to *trans*-$[RuCl(pdma)_2(MeCN)]^+$.[8] Under the same conditions the dimer **5** is photostable.

Electrochemical studies

All of the complexes were studied by cyclic voltammetry in acetonitrile or dimethylformamide (dmf) and results, together with data for *trans*-$[RuCl(pdma)_2(pyz)]PF_6$,[8] are presented in Table 2. All except **10** exhibit reversible or quasi-reversible (ΔE_p > 70 mV) $Ru^{III/II}$ oxidation waves at potentials which are in accord with expectation. Deprotonation of **6** to give **7** produces a shift of −0.38 V in the $Ru^{III/II}$ reduction potential as the neutral, S-bound pyridine-4-thione ligand is converted into the pyridine-4-thiolate anion. Both **6** and **7** show several irreversible oxidation waves above +1.0 V which give rise to product waves on return scanning. Complex **10** shows several irreversible oxidation waves, accompanied by displaced cathodic waves, indicating complicated ligand- and metal-based oxidation behaviour.

Reversible ligand-based reduction processes are also observed for salts **1**, **3** and **11**, although scanning too far negative destroys the reversibility of this wave for **11**. Salt **12** shows several irreversible reduction waves between −1.1 and −1.6 V.

The extent of ligand-mediated, intermetallic electronic coupling can be assessed by examination of the voltammograms for the dinuclear complexes. In the pyrazine-bridged dimer **1** a separation between the two $Ru^{III/II}$ waves ($\Delta E_{\frac{1}{2}}$) of 320 mV indicates an extensive degree of coupling. This is intermediate between the $\Delta E_{\frac{1}{2}}$ values of 280 and 390 mV reported for the related complexes *trans*-$[\{RuCl(py)_4\}_2(\mu\text{-pyz})]^{2+}$ (ref. 6) and $[\{Ru(NH_3)_5\}_2(\mu\text{-pyz})]^{5+}$ (ref. 1) (in aqueous solution), respectively.

The only other new dinuclear complex which clearly shows two $Ru^{III/II}$ waves is the fmn-bridged dimer **5**, for which $\Delta E_{\frac{1}{2}}$ is *ca*. 100 mV. The 4,4′-bipy-bridged dimer **3** shows a single wave, with a slightly increased ΔE_p indicative of two very close one-electron oxidations. This is confirmed by a peak current which is twice that of the 4,4′-bipy reduction wave. The bpe-bridged dimer **12** shows a single oxidation wave with no evidence for any Ru–Ru interaction. The trend of increasing ligand-mediated coupling in the order bpe < 4,4′-bipy < fmn < pyz follows that observed previously in $\{Ru(NH_3)_5\}^{n+}$ (n = 2 or 3) dinuclear complexes.[4]

The dpds-bridged dimer **13** was investigated with the expectation that a strong interaction between the ruthenium centres would give rise to two, well separated $Ru^{III/II}$ oxidation processes, as has been reported for $[\{Ru(NH_3)_5\}_2(\mu\text{-dpds})]^{4+}$ ($\Delta E_{\frac{1}{2}}$ = 290 mV).[19] Although electrochemical data for the triiodide anion in dmf solution are unavailable, the irreversible and quasi-reversible waves at 0.43 and 0.66 V *vs*. SCE for **13** can reasonably be assigned to the redox couples $I_3^- + 2e^- \rightleftharpoons 3I^-$ and $3I_2 + 2e^- \rightleftharpoons 2I_3^-$, respectively.[21] The quasi-reversible wave at 1.12 V *vs*. SCE ascribed to a $Ru^{III/II}$ oxidation is at almost the same potential as that for the mononuclear analogue **9**. The origin of the irreversible oxidation at 1.52 V *vs*. SCE is uncertain, but is considered unlikely to be a second $Ru^{III/II}$ oxidation process. It hence appears that the two ruthenium centres in **13** do not interact as strongly as do those in $[\{Ru(NH_3)_5\}_2(\mu\text{-dpds})]^{4+}$, but the reasons for this marked difference in behaviour are unclear.

Structural studies

Single-crystal structures were obtained for salts **1**·2MeCN·Et_2O, **3**·2MeCN·Et_2O, **6** and **13**·2MeCN. Representations of the cations are shown in Figs. 1, 2, 3 and 4, respectively. All of the complexes show the expected *trans* arrangement of the pdma ligands, with typical values for Ru–As bond lengths and As–Ru–As chelate angles.[8]

In salts **1**·2MeCN·Et_2O and **3**·2MeCN·Et_2O the pyrazine or pyridyl ring planes approximately bisect the As–Ru–As chelate angles, presumably in order to minimize steric interactions with the methyl groups. Both of the complex cations possess a centre of symmetry at the centre of the bridging ligand, causing the two *trans*-$\{Ru(pdma)_2\}^{2+}$ units to be eclipsed. The pdma ligands distort slightly away from the bridging ligands, with average As–Ru–N angles of 92.7(3) and 92.26(9)° for **1**·2MeCN·Et_2O and **3**·2MeCN·Et_2O, respectively. Of the small number of structurally characterized 4,4′-bipy-bridged dinuclear transition-metal complexes most contain Cu^I or Cu^{II}.[22] The ligand can adopt either a planar or twisted conformation. Many 4,4′-bipy-bridged diruthenium complexes have been

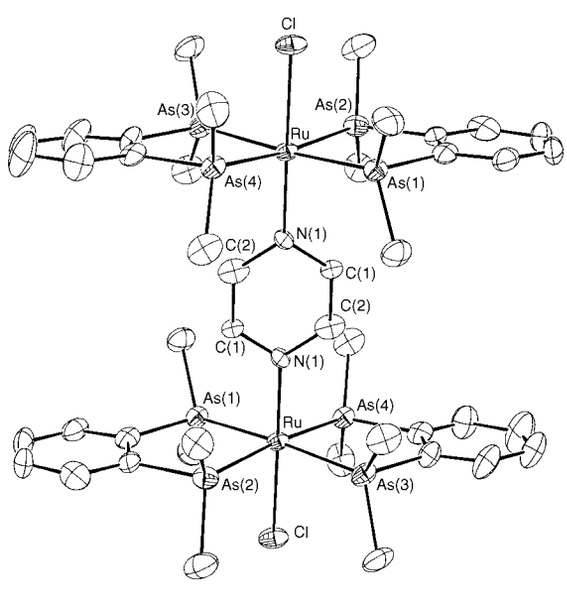

Fig. 1 An ORTEP[16] representation of the cation in salt **1**·2MeCN·Et_2O, *trans*-$[\{RuCl(pdma)_2\}_2(\mu\text{-pyz})]^{2+}$, with hydrogen atoms omitted

Table 3 Crystallographic data and refinement details for salts **1**·2MeCN·Et_2O, **3**·2MeCN·Et_2O, **6** and **13**·2MeCN

	1·2MeCN·Et_2O	**3**·2MeCN·Et_2O	**6**	**13**·2MeCN
Formula	$C_{52}H_{84}As_8Cl_2F_{12}N_4OP_2Ru_2$	$C_{58}H_{72}As_8Cl_2F_{12}N_4OP_2Ru_2$	$C_{25}H_{37}As_4ClF_6NPRuS$	$C_{54}H_{78}As_8Cl_2I_6N_4Ru_2S_2$
M	1943.59	2003.58	964.81	2481.12
Crystal system	Monoclinic	Orthorhombic	Orthorhombic	Monoclinic
Space group	$C2/c$	$Pccn$	$P2_12_12_1$	$Fdd2$
a/Å	24.258(3)	14.8130	11.666(3)	29.972(3)
b/Å	17.4729(22)	32.0660	27.953(8)	52.151(4)
c/Å	18.6911(19)	16.5620	10.730(3)	9.9796(10)
β/°	95.679(10)			
U/Å^3	7883.5(16)	7866.8457	3499(2)	15599(3)
Z	4	4	4	8
D_c/Mg m^{-3}	1.638	1.692	1.831	2.113
T/K	153	107	291	173(2)
λ/Å	0.710 73 (Mo-Kα)	0.710 73 (Mo-Kα)	0.710 73 (Mo-Kα)	0.710 73 (Mo-Kα)
F(000)	3816.67	3920.00	1888	9328
μ/mm^{-1}	3.87	3.899	4.414	6.287
Scan type	ω	φ	ω	φ
2θ limit/°	46.0	56.6	50.1	50.0
h, k, l Ranges	−26 to 26, 0–19, 0–20	0–19, 0–38, −20 to 0	0–13, 0–33, 0–12	−35 to 35, −43 to 61, −11 to 11
Reflections collected	5538	77750	3522	18413
Unique reflections (R_{int})	5507 (0.015)	9730 (0.055)	3522	6302 (0.0563)
Observed reflections	3569 [$I > 2.5\sigma(I)$]	7417 [$I > 3\sigma(I)$]	2294 [$I > 3\sigma(I)$]	6301 [$I > 2\sigma(I)$]
Final R indices*	$R = 0.055$, $R' = 0.075$	$R = 0.0439$, $R' = 0.0486$	$R = 0.041$, $R' = 0.037$	$R1 = 0.0457$, $wR2 = 0.0923$
(all data)*	$R = 0.106$, $R' = 0.080$	$R = 0.0527$, $R' = 0.0496$	$R = 0.0935$, $R' = 0.0431$	$R1 = 0.0564$, $wR2 = 0.0987$
Goodness of fit, S	2.16	2.96	1.58	1.148
No. parameters	375	394	361	361
Peak and hole/e Å^{-3}	2.050, −0.680	1.34, −1.59	0.69, −0.51	1.25, −1.07

* For salts **1**·2MeCN·Et_2O, **3**·2MeCN·Et_2O and **6**, $R = \Sigma(||F_o| - |F_c||)/\Sigma|F_o|$, $R' = [\Sigma w(F_o - F_c)^2/\Sigma wF_o^2]^{\frac{1}{2}}$, $S = [\Sigma w(F_o - F_c)^2/(N_o - N_p)]^{\frac{1}{2}}$ where N_o = number of reflections, N_p = number of parameters and $w = 4F_o^2/\sigma^2(F_o^2)$. For **13**·2MeCN, $R1 = \Sigma(||F_o| - |F_c||)/\Sigma|F_o|$, $wR2 = [\Sigma w(F_o^2 - F_c^2)^2/\Sigma w(F_o^2)^2]^{\frac{1}{2}}$, $S = [\Sigma w(F_o^2 - F_c^2)^2/(N_o - N_p)]^{\frac{1}{2}}$, $w^{-1} = [\sigma^2(F_o^2) + (0.0241\,P)^2 + 470\,P]$ and $P = [\max(F_o^2, 0) + 2F_c^2]/3$.

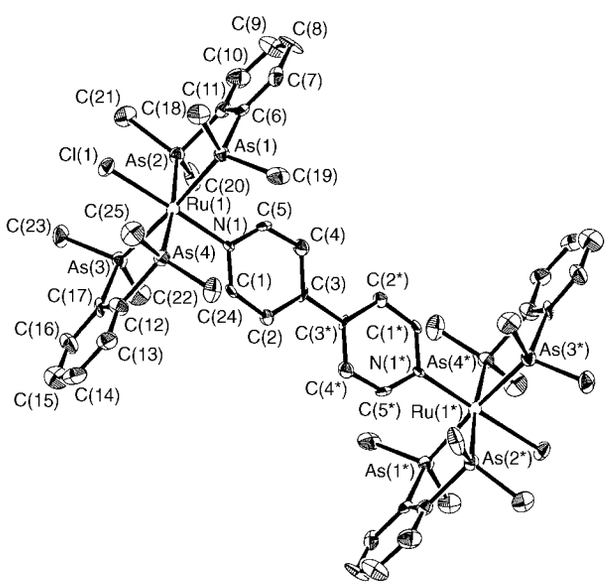

Fig. 2 An ORTEP[16] representation of the cation in salt **3**·2MeCN·Et_2O, *trans*-[{RuCl(pdma)$_2$}$_2$(μ-4,4′-bipy)]$^{2+}$, with hydrogen atoms omitted

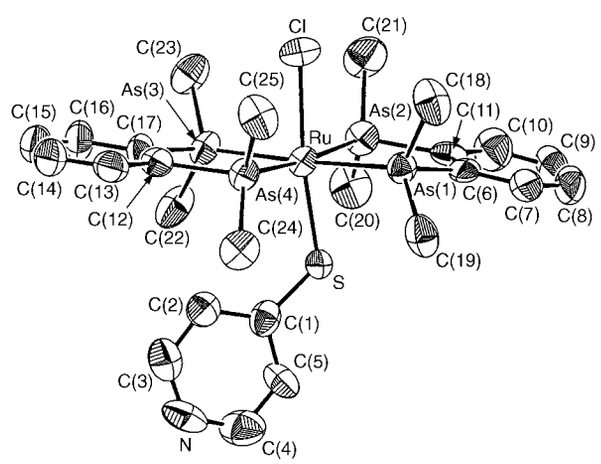

Fig. 3 An ORTEP[16] representation of the cation in salt **6**, *trans*-[RuCl(pdma)$_2$(C_5H_5NS)]$^+$, with hydrogen atoms omitted

investigated for their electronic properties, but **3**·2MeCN·Et_2O appears to be the first to be structurally characterized. The planarity of the 4,4′-bipy bridge in **3**·2MeCN·Et_2O indicates that the steric repulsions between the 2,2′ and 6,6′ hydrogens are overcome by electronic and crystal-packing factors.

The C–S bond length of 1.68(2) Å in complex **6** corresponds to a C=S double bond, as expected for the thione form of the ligand. No other reported structures of complexes containing the pyridine-4-thione ligand are available for comparison. The overall structure of the pyridine-4-thione moiety is very similar to that found in the free thione and in a crown ether derivative in which the C–S bond lengths are 1.703(2) and 1.690(4) Å, respectively.[23,24] The Ru–S bond length of 2.343(4) Å is normal, but the Ru–S–C angle of 122.2(6)° is somewhat larger than those previously reported for ruthenium(II) complexes of monodentate thiones. Typical angles lie in the range 112–116°,[25] with the largest reported being 119.1(1)° in [Ru{SC(NH_2)$_2$}$_6$][CF_3SO_3]$_2$.[25b] Since the pyridyl ring plane in **6** approximately bisects one of the As–Ru–As chelate angles it is likely that the increased Ru–S–C angle reflects a slight steric interaction with one of the pdma ligands. The strong *trans* influence of the σ-donating thione moiety leads to a long Ru–Cl bond length of 2.441(4) Å.

As in salts **1**·2MeCN·Et_2O and **3**·2MeCN·Et_2O, the pyridyl ring planes in **13**·2MeCN approximately bisect the As–Ru–As chelate angles. The complex adopts the expected folded conformation, with a crystallographic two-fold axis perpendicular to the centre of the S–S bond. The C–S–S angle is 104.1(4)°, the C–S–S–C torsion angle is 86.6° and the angle between the normals to the pyridyl rings is 72.7°. Neither the structure of dpds nor of any of its complexes have been reported, but the dimensions of the dpds bridge in **13**·2MeCN are very similar to those of di-2-pyridyl disulfide and related diaryl disulfides.[26]

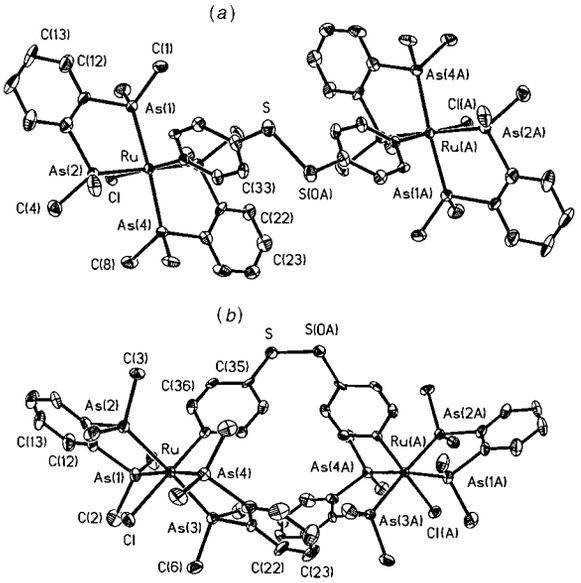

Fig. 4 Two alternative ORTEP[16] representations of the cation in salt **13**·2MeCN, *trans*-[{RuCl(pdma)$_2$}$_2$(μ-dpds)]$^{2+}$, with hydrogen atoms omitted

Table 4 Selected bond distances (Å) and angles (°) for salt **1**·2MeCN·Et$_2$O

Ru–As(1)	2.427(2)	Ru–As(4)	2.425(2)
Ru–As(2)	2.433(2)	Ru–Cl	2.429(4)
Ru–As(3)	2.432(2)	Ru–N(1)	2.066(10)
As(1)–Ru–As(2)	84.83(6)	As(2)–Ru–N(1)	93.3(3)
As(1)–Ru–As(3)	175.47(7)	As(3)–Ru–As(4)	84.49(6)
As(1)–Ru–As(4)	94.24(6)	As(3)–Ru–Cl	88.38(10)
As(1)–Ru–Cl	87.22(10)	As(3)–Ru–N(1)	92.5(3)
As(1)–Ru–N(1)	91.9(3)	As(4)–Ru–Cl	87.16(11)
As(2)–Ru–As(3)	95.95(6)	As(4)–Ru–N(1)	93.0(3)
As(2)–Ru–As(4)	173.62(7)	Cl–Ru–N(1)	179.2(3)
As(2)–Ru–Cl	86.49(11)		

Table 5 Selected bond distances (Å) and angles (°) for salt **3**·2MeCN·Et$_2$O

Ru(1)–As(1)	2.4237(5)	Ru(1)–As(4)	2.4230(5)
Ru(1)–As(2)	2.4213(5)	Ru(1)–Cl(1)	2.431(1)
Ru(1)–As(3)	2.4220(5)	Ru(1)–N(1)	2.111(3)
As(1)–Ru(1)–As(2)	84.74(2)	As(2)–Ru(1)–N(1)	91.76(9)
As(1)–Ru(1)–As(3)	176.26(2)	As(3)–Ru(1)–As(4)	85.37(2)
As(1)–Ru(1)–As(4)	95.80(2)	As(3)–Ru(1)–Cl(1)	87.95(3)
As(1)–Ru(1)–Cl(1)	88.58(3)	As(3)–Ru(1)–N(1)	91.87(9)
As(1)–Ru(1)–N(1)	91.59(9)	As(4)–Ru(1)–Cl(1)	86.45(3)
As(2)–Ru(1)–As(3)	93.75(2)	As(4)–Ru(1)–N(1)	93.80(9)
As(2)–Ru(1)–As(4)	174.39(2)	Cl(1)–Ru(1)–N(1)	179.68(9)
As(2)–Ru(1)–Cl(1)	87.98(3)		

Table 6 Selected bond distances (Å) and angles (°) for salt **6**

Ru–As(1)	2.416(2)	Ru–Cl	2.441(4)
Ru–As(2)	2.413(2)	Ru–S	2.343(4)
Ru–As(3)	2.407(2)	S–C(1)	1.68(2)
Ru–As(4)	2.410(2)		
As(1)–Ru–As(2)	84.56(7)	As(2)–Ru–S	86.4(1)
As(1)–Ru–As(3)	176.74(7)	As(3)–Ru–As(4)	85.51(7)
As(1)–Ru–As(4)	95.17(7)	As(3)–Ru–Cl	87.1(1)
As(1)–Ru–Cl	89.8(1)	As(3)–Ru–S	98.4(1)
As(1)–Ru–S	84.7(1)	As(4)–Ru–Cl	86.0(1)
As(2)–Ru–As(3)	94.47(7)	As(4)–Ru–S	98.9(1)
As(2)–Ru–As(4)	174.72(8)	Cl–Ru–S	172.9(1)
As(2)–Ru–Cl	88.7(1)	Ru–S–C(1)	122.2(6)

Table 7 Selected bond distances (Å) and angles (°) for salt **13**·2MeCN

Ru–As(1)	2.4339(14)	Ru–Cl	2.438(3)
Ru–As(2)	2.4264(13)	Ru–N(31)	2.113(8)
Ru–As(3)	2.4124(13)	S–C(34)	1.765(11)
Ru–As(4)	2.4218(13)	S–S^{I}	2.029(6)
As(1)–Ru–As(2)	85.36(5)	As(2)–Ru–N(31)	92.3(2)
As(1)–Ru–As(3)	94.57(5)	As(3)–Ru–As(4)	85.08(5)
As(1)–Ru–As(4)	173.68(5)	As(3)–Ru–Cl	89.04(8)
As(1)–Ru–Cl	86.18(8)	As(3)–Ru–N(31)	91.3(2)
As(1)–Ru–N(31)	93.6(2)	As(4)–Ru–Cl	87.50(8)
As(2)–Ru–As(3)	176.36(5)	As(4)–Ru–N(31)	92.8(2)
As(2)–Ru–As(4)	94.60(5)	Cl–Ru–N(31)	179.6(2)
As(2)–Ru–Cl	87.33(8)	C(34)–S–S^{I}	104.1(4)

Symmetry transformation used to generate equivalent atoms: I $-x-\frac{1}{2}, -y+\frac{1}{2}, z$.

Conclusion

The precursor *trans*-[RuCl(pdma)$_2$(NO)][PF$_6$]$_2$ acts as a useful source of symmetrical dinuclear complexes *trans*-[{RuCl(pdma)$_2$}$_2$(μ-L–L)]$^{2+}$ where L–L is a neutral bridging ligand. The extent of intermetallic electronic coupling in these complexes, as probed by cyclic voltammetry, follows that observed in {Ru(NH$_3$)$_5$}$^{n+}$ ($n = 2$ or 3) dinuclear complexes, with the exception of L–L = dpds. Further studies with the new dimers involve investigations of the mixed-valence properties of their one-electron oxidized forms, and of their derivatization by chloride substitution.

Acknowledgements

Thanks are due to the Nuffield Foundation for financial support and to Johnson Matthey plc for a generous loan of ruthenium trichloride.

References

1 C. Creutz and H. Taube, *J. Am. Chem. Soc.*, 1973, **95**, 1086.
2 C. Creutz, *Prog. Inorg. Chem.*, 1983, **30**, 1.
3 R. J. Crutchley, *Adv. Inorg. Chem.*, 1994, **41**, 273.
4 M. D. Ward, *Chem. Soc. Rev.*, 1995, **24**, 121.
5 R. W. Callahan, F. R. Keene, T. J. Meyer and D. J. Salmon, *J. Am. Chem. Soc.*, 1977, **99**, 1064.
6 B. J. Coe, T. J. Meyer and P. S. White, *Inorg. Chem.*, 1995, **34**, 593.
7 B. J. Coe, T. J. Meyer and P. S. White, *Inorg. Chem.*, 1995, **34**, 3600.
8 B. J. Coe, M. Chery, R. L. Beddoes, H. Hope and P. S. White, *J. Chem. Soc., Dalton Trans.*, 1996, 3917.
9 P. G. Douglas, R. D. Feltham and H. G. Metzger, *J. Am. Chem. Soc.*, 1971, **93**, 84.
10 E. J. Gabe, Y. Le Page, J.-P. Charland, F. L. Lee and P. S. White, *J. Appl. Crystallogr.*, 1989, **22**, 384.
11 P. T. Beurskens, G. Admiraal, G. Buerskens, W. P. Bosman, R. de Gelder, R. Israel and J. M. M. Smits, The DIRDIF 94 program system, Technical Report of the Crystallography Laboratory, University of Nijmegen, 1994.
12 TEXSAN-TEXRAY Structure Analysis Package, Molecular Structure Corporation, Houston, TX, 1985 and 1992.
13 G. M. Sheldrick, SHELXS 86, *Acta Crystallogr., Sect. A*, 1990, **46**, 467.
14 N. P. C. Walker and D. Stuart, *Acta Crystallogr., Sect. A*, 1983, **39**, 158.
15 SHELXTL 5.03 program system, Siemens Analytical X-Ray Instruments, Madison, WI, 1995.
16 C. K. Johnson, ORTEP, a Fortran thermal ellipsoid plot program, Technical report ORNL-5138, Oak Ridge National Laboratory, Oak Ridge, TN, 1976.
17 A. R. Katritzky, M. Karelson and P. A. Harris, *Heterocycles*, 1991, **32**, 329; J. A. Joule, K. Mills and G. F. Smith, *Heterocyclic Chemistry*, Chapman and Hall, London, 3rd edn., 1995.
18 R. M. Berger and D. D. Ellis, II, *Inorg. Chim. Acta*, 1996, **241**, 1 and refs. therein.
19 I. de Sousa Moreira and D. W. Franco, *Inorg. Chem.*, 1994, **33**, 1607.

20 B. P. Kennedy and A. B. P. Lever, *Can. J. Chem.*, 1972, **50**, 3488.
21 G. Milazzo and S. Caroli, *Tables of Standard Electrode Potentials*, Wiley, New York, 1978, pp. 292 and 293.
22 A. S. Batsanov, M. J. Begley, P. Hubberstey and J. Stroud, *J. Chem. Soc., Dalton Trans.*, 1996, 1947 and refs. therein.
23 M. C. Etter, J. C. MacDonald and R. A. Wanke, *J. Phys. Org. Chem.*, 1992, **5**, 191.
24 J. S. Bradshaw, P. Huszthy, H. Koyama, S. G. Wood, S. A. Strobel, R. B. Davidson, R. M. Izatt, N. K. Dalley, J. D. Lamb and J. J. Christensen, *J. Heterocycl. Chem.*, 1986, **23**, 1837.
25 (*a*) P. Mura, B. G. Olby and S. D. Robinson, *Inorg. Chim. Acta*, 1985, **97**, 45; (*b*) G. Douglas, K. W. Muir, A. Patel and D. T. Richens, *Acta Crystallogr., Sect. C*, 1991, **47**, 1394; (*c*) W. A. Schenk, T. Stur and E. Dombrowski, *Inorg. Chem.*, 1992, **31**, 723; *J. Organomet. Chem.*, 1994, **472**, 257; (*d*) U. Bierbach, W. Barklage, W. Saak and S. Pohl, *Z. Naturforsch., Teil B*, 1992, **47**, 1593; (*e*) C. D. Bryan, A. W. Cordes and M. Draganjac, *Acta Crystallogr., Sect. C*, 1994, **50**, 1231.
26 N. V. Raghavan and K. Seff, *Acta Crystallogr., Sect. B*, 1977, **33**, 386.

Received 21*st August* 1996; *Paper* 6/05834E